JOURNAL OF APPLIED ELECTROCHEMISTRY **27** (1997) 1088–1094

Zinc–cobalt alloy electrodeposition from chloride baths

R. FRATESI, G. ROVENTI, G. GIULIANI,

Dipartimento di Scienze dei Materiali e della Terra, Università di Ancona, via Brecce Bianche, 60131 Ancona, Italy

C. R. TOMACHUK

Departamento de Engenharia de Materiais, Faculdade de Engenharia Mecânica, Universidade Estadual de Campinas, CEP 13081-970, C.P. 6122 Campinas, São Paulo, Brazil

Received 29 July 1996; revised 21 November 1996

Electrodeposition of Zn–Co alloys on iron substrate from chloride baths under galvanostatic and potentiostatic conditions were carried out. Current density, temperature and cobalt percentage in the bath were found to strongly influence the composition of the deposits and their morphology. Changes in potentials, current efficiency and partial current densities were studied. The results show that the shift in potential and in the cobalt percentage of the deposits, for a particular current density during galvanostatic electrodeposition, does not always correspond to the transition from normal to anomalous codeposition. This shift is attributed to zinc ion discharge, which passes from underpotential to thermodynamic conditions. In the range of potentials for the underpotential deposition of zinc, the electrodeposition of zinc–cobalt alloys is discussed, emphasizing the influence of the electrode potential on the composition and microstructure of the deposits.

1. Introduction

The electrodeposition of Zn alloys with group eight metals (Ni, Co and Fe) has recently been attracting interest because of the high corrosion resistance compared to that of pure zinc. The electrodeposition of these alloys is considered a codeposition of anomalous type, according to the Brenner definition [1]; that is, the less noble metal deposits preferably on the cathode with respect to the more noble one. The operating conditions such as current density, temperature, pH, organic additives, buffer capacity, concentration of all solution components etc. lead to changes in the kinetics of electrodeposition, composition and morphology of the coatings, as well as changes in their physico-mechanical characteristics [2–7]. Therefore, normal codeposition is possible, even in particular electrodeposition conditions [8].

Several hypotheses have been advanced to explain the anomalous codeposition of alloys. The ideas are focused on phenomena occurring on the cathode surface. Dahms and Croll [9], who studied the anomalous electrodeposition of Fe–Ni alloy, concluded that the discharge of nickel is hindered by the formation of ferrous hydroxide on the electrode surface. Higashi *et al.* and Decroly [2, 10, 11] proposed the hydroxide suppression mechanism to explain the anomalous codeposition of Zn–Co alloy in a sulfate bath. The discharge of the cobalt is inhibited by the formation of a zinc hydroxide film which offers resistance to the transport of the Co^{2+} ions. On the contrary $Co(OH)_2$ is not formed because the pH does not reach a critical value for precipitation.

However, not all researchers agree on this mechanism. Nicol and Philip [12] suggested that underpotential deposition (UPD) of the less noble metal on the cathode surface suppresses the deposition of the more noble metal. The term 'underpotential deposition' is used for the deposition of metal species on a foreign substrate in a potential region which is more positive than the equilibrium potential of the bulk deposit. Swathirajan [13] found that the strong inhibition of nickel deposition in the Zn–Ni alloy electrodeposition is due to submonolayer amounts of underpotential deposited zinc.

Previously [3, 8, 14], anomalous codeposition of Zn–Ni and Zn–Co alloys has been treated, emphasizing the importance of the kinetic parameters of the cathodic reactions: the iron group metals are generally characterized by very low exchange current densities and reflect 'electrochemical inertia' [15], unlike zinc, which shows high exchange current density. By studying the electrodeposition of Zn–Ni alloys from baths containing NH_4Cl, no increase in the partial current of hydrogen reduction was observed at the potential values from which anomalous codeposition begins; this fact, plus the formation of zinc ammonium complexes, seems to exclude the precipitation of zinc hydroxide at the electrode surface. These results are supported by Mathias *et al.* [16, 17]. They found that, on using the Roehl bath (pH 1.6), the electrodeposition of Zn–Ni alloys is anomalous even though the hydrogen current is not high enough to raise the interfacial pH much above the bulk pH, as would be necessary for the formation of $Zn(OH)_2$. These authors calculated that the zinc

0021-891X

exchange current density is five orders of magnitude higher than that of nickel and attributed the anomalous codeposition to the intrinsically slow nickel kinetics.

In the present work, the codeposition of Zn–Co alloys from a chloride bath has been studied. The bath was free of additives such as levellers or brighteners since they can strongly influence the composition and the morphology of the alloys deposited on the cathode.

2. Experimental details

Zn–Co alloys were obtained at various temperatures (25, 40 and 55 °C), under galvanostatic and potentiostatic conditions using baths of the following composition: $ZnCl_2$ 31.1–70.0 g dm^{-3}; $CoCl_2 \cdot 6H_2O$ 90.7–15.2 g dm^{-3} (M_{tot} 37.4 g dm^{-3}); H_3BO_3 26 g dm^{-3}; KCl 220 g dm^{-3} (pH 4.3, 4.2 and 3.9 for baths with Co 10, 30 and 60%, respectively). Boric acid is used extensively in Zn–Co and Zn–Ni alloy electrodepositions, as a buffer to prevent the pH rise at the electrode surface; however, the function of H_3BO_3 is a controversial subject [18, 19]. Tests with only cobalt or zinc, maintaining the total metal quantity and the other components of the bath constant, were also carried out. Solutions were prepared with doubly distilled water and analytical grade reagents.

Electrodeposits were obtained on both sides of mild steel discs, 1 mm thick (exposed area 15 cm^2). Before electrodeposition, the samples were smoothed with emery paper and any grease was removed from their surface by anodic and cathodic electrolysis for 2 min in an aqueous NaOH 60 g dm^{-3} solution at 4 V against graphite anodes. The samples were then neutralized in a 2% HCl solution and rinsed with distilled water.

A PVC cell 1 dm^3 in capacity was used. The steel cathode was centrally positioned, whereas two zinc anodes (total area 150 cm^2) were symmetrically positioned with respect to the central cathode. Before immersion in the bath, the zinc anodes were immersed for 3 h without current flow, in a solution of similar composition at 40 °C. The zinc sheets were coated with a dark cobalt layer, so avoiding the depletion of cobalt in the bath due to its cementation on the zinc anodes. Cathode potential measurements were performed during electrodeposition using a Ag/AgCl reference electrode. Polarization was applied when the cathode was immersed in the bath and electrolysis was continued until deposits at least 6 μm thick were obtained. During the electrodeposition, the cathodic solution was mechanically stirred. The amount of electrical charge during potentiostatic tests was registered by means of a coulometer AMEL model 731. At the end of each deposition, the disc cathodes were thoroughly washed with water and then ethanol, hot air dried and weighed.

To determine the percentage composition of the electrodeposited alloys, the deposits were stripped in a minimum volume of 1:3 HCl solution and analysed for cobalt and zinc by means of inductively coupled plasma spectroscopy (ICPS). By means of Faraday's law, the partial currents of zinc and cobalt were calculated and their respective polarization curves were plotted.

The morphology of the deposits was observed by means of scanning electron microscopy (SEM). The deposited phases were analysed by X-ray diffraction with CuK_α ($\lambda = 15.4$ nm) and identified by powder diffraction file card (JCPDS).

All the tests were repeated three times with good agreement of the results.

3. Results and discussion

The data shown in Fig. 1 were obtained by galvanostatic electrodeposition at 25 °C. They show the influence of current density on the chemical composition of the deposits obtained from baths containing different percentages of cobalt ions. The percentage of Co present in the baths and deposits, indicated by Co_b and Co_d was calculated as follows:

$$\mathrm{Co}/\% = \frac{\mathrm{Co}/\,\mathrm{g}}{(\mathrm{Co}+\mathrm{Zn})/\mathrm{g}} \times 100$$

The trend of the curves is similar to that already known for codepositions of anomalous type [2, 8]: the percentage of cobalt deposited on the cathode depends on the cobalt/zinc concentration ratio in the bath and is quite constant for a large range of current density, where the deposition of zinc and cobalt is of anomalous type. At low current densities the percentage of cobalt in the deposits increases abruptly reaching values of almost 100% and the codeposition becomes normal. The value of current density corresponding to the transition from normal to anomalous codeposition is called the transition current density (i_T) and it depends, at constant temperature, on the bath chemical composition. In Fig. 1 the letters (a), (b) and (c) show the points of the respective curves where the percentage of cobalt in the deposits is equal

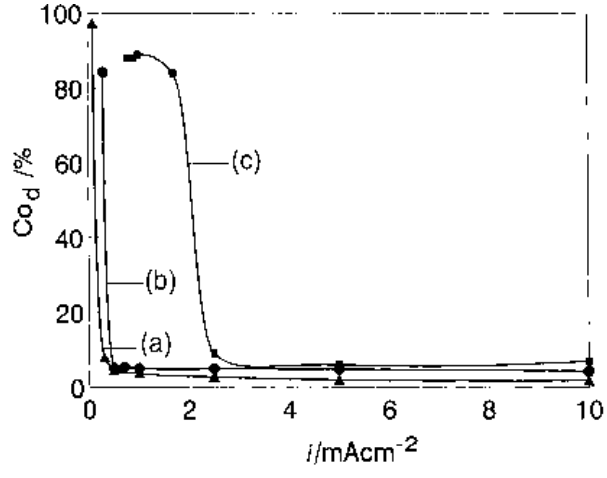

Fig. 1. Effect of current density on the percentage of cobalt in zinc–cobalt alloys electrodeposited from bath containing the following percentages of cobalt: (▲) 10%, (●) 30%, (■) 60%. $T = 25$ °C.

to that in the bath; the 'imaginary' line interpolating the three points represents the composition reference line (CRL). With increase in cobalt/zinc concentration ratio, a higher current density is necessary for anomalous deposition to occur.

The temperature strongly affects the composition of the deposits, as shown in Fig. 2. On increasing the temperature, the sharp decrease in cobalt percentage in the coatings occurs at higher current densities and this is associated with the abrupt shift of cathodic potential toward more negative values. At temperatures of 25 and 40 °C the transition from normal to anomalous codeposition (points A and B in Fig. 2) corresponds to the rapid shift in the cobalt percentage of the deposits and in the cathodic potentials. In the Zn–Co electrodeposition carried out at 55 °C, at about 3.6 mA cm^{-2} the cobalt percentage of the deposits decreases abruptly, but it still remains higher than the cobalt percentage in the bath. In spite of the sharp shift in cathodic potential, normal/anomalous transition does not take place. This behaviour is more evident in the electrodeposition carried out at 55 °C, but in a solution with a cobalt ion concentration of 60% (Fig. 3). In this case the characteristic shift in the cathodic potential, as well as the reduction in cobalt percentage of the deposits at about 35 mA cm^{-2}, are still less marked and the codeposition always remains normal even at relatively high current densities (50 mA cm^{-2}). The alloy current efficiency is almost 100% and therefore the current efficiency of hydrogen is very low throughout the whole current density range studied. Figures 2 and 3 show that only for some experimental conditions does the shift in potential and in the cobalt percentage of deposits correspond to the transition from normal to anomalous electrodeposition. Only in these latter cases, the current density corresponding to the sharp shift in cathodic potential is the transition current.

Figure 4 shows the polarization curves obtained by galvanostatic tests at 55 °C using baths containing different cobalt/zinc concentration ratios. The curves

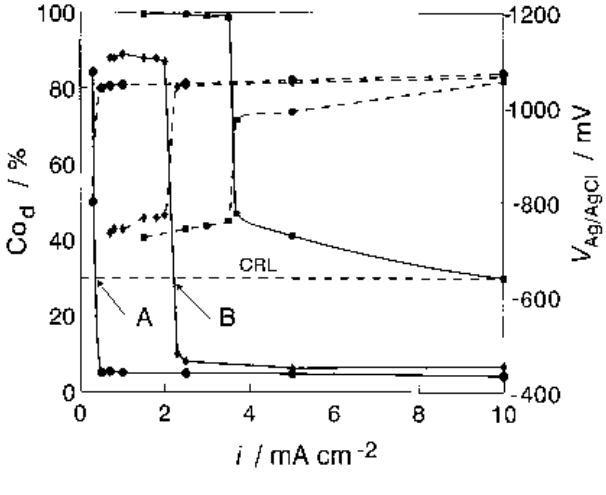

Fig. 2. Polarization curves during alloy deposition (- - - -) and effect of current density on the cobalt content of deposits (——) at the following temperatures: (●) 25 °C, (◆) 40 °C, (■) 55 °C. Co_b 30%.

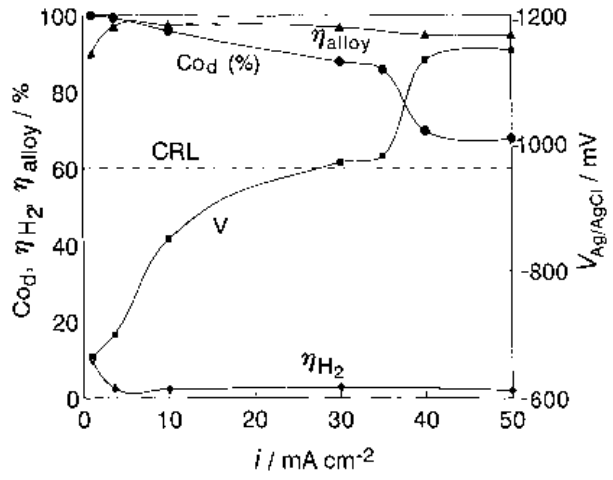

Fig. 3. Polarization curve during alloy deposition (V) and effect of current density on cobalt content of deposits (Co_d), on current efficiency for alloy deposition (η_{alloy}) and current efficiency for hydrogen reduction (ηH_2). Co_b 60%; $T = 55$ °C.

obtained from the baths containing only zinc or cobalt ions are also indicated. The cobalt deposition from the solution containing only cobalt ions starts at about −550 mV, while the zinc deposition from baths containing only zinc ions starts at about −1000 mV. The alloy polarization curves are close to the curve for Co at low current densities, while they are very close to the curve for Zn after the rapid shift in potential. The sharp variations in cathodic potential are due to the zinc ions discharge which passes from underpotential to thermodynamic conditions. The galvanostatic tests do not shed light on the phenomena that occur on the electrode in the range in which the potential rapidly changes.

Therefore, potentiostatic electrodeposition was carried out in the current range where the cathodic potential is unstable (Fig. 5). The curves related to pure zinc or pure cobalt are similar to those obtained by galvanostatic tests. The zinc and the cobalt ions separately begin deposition only at their respective equilibrium potential of the bulk deposit. The curves

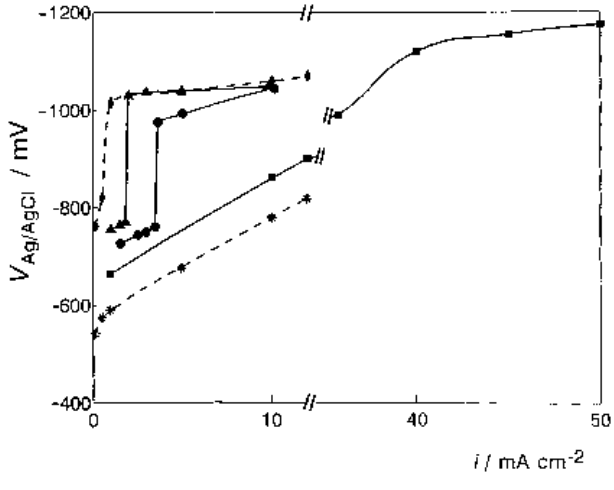

Fig. 4. Polarization curves for zinc, zinc–cobalt alloys and cobalt galvanostatic electrodeposition from baths containing the following percentages of cobalt: (◆) 0%, (▲) 10%, (●) 30%, (■) 60%, (✳) 100%. $T = 55$ °C.

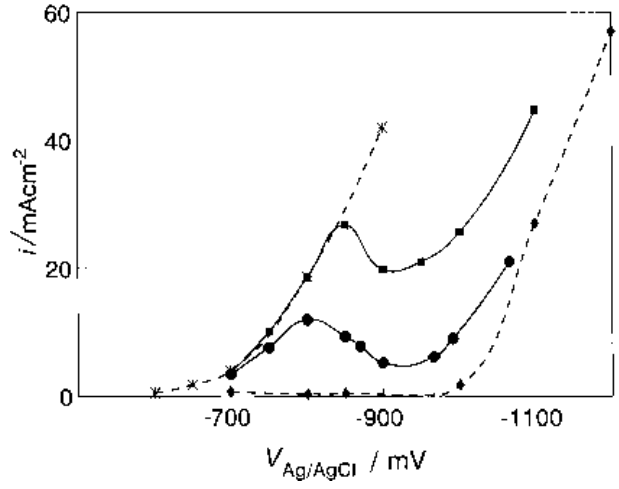

Fig. 5. Polarization curves for zinc, zinc-cobalt alloys and cobalt potentiostatic electrodeposition from baths containing the following percentages of cobalt: (◆) 0%, (●) 30%, (■) 60%, (✳) 100%. $T = 55\,°C$.

due to the deposition of Zn–Co alloys, compared to those of galvanostatic type, are more detailed. At more positive potential values the curves are similar to those of pure cobalt deposition, but around –800 to –850 mV the current significantly drops and then, at potential values more negative than –950 mV it again sharply increases.

The total electrolysis current together with the partial currents related to cobalt, zinc and hydrogen and also the zinc percentage in the alloy deposit obtained in the potential range –660 to –1100 mV are shown in Fig. 6. In the operating conditions related to Fig. 6, the trend of the current density due to the alloy is quite similar to the partial current density of cobalt up to about –800 mV, and the deposits contain more than 90% of cobalt in the range –600 to –800 mV. The zinc deposition starts around –700 mV and its percentage in the deposits increases as the cathodic potential change toward more negative values. The zinc reduction in this field of potential is assisted by the presence of cobalt ions in the solution, indeed the partial current density of zinc depends on the percentage of cobalt in the bath, when the other experimental conditions are kept constant (Fig. 7); a connection between i_{Co} and i_{Zn} was found previously, though for different experimental conditions [20]. How the cobalt supports the underpotential electrodeposition of zinc is not clear at the moment. At a potential of –800 mV vs Ag/AgCl, the percentage of zinc in the deposits is about 14% and the partial current density of cobalt reaches a maximum value; at –830 mV the percentage of zinc in the deposits reaches 19% and the partial current densities of cobalt and of zinc begin to decrease. The zinc percentage in the deposits remains quite constant until about –900 mV ($Zn_d \sim 23\%$), then it rapidly begins to increase again together with the partial current of zinc (i_{Zn}). The cathodic reduction of zinc prevails over cobalt reduction only at potential values more negative than about –970 mV, where it begins to discharge in thermodynamic conditions. In these conditions, however, the codeposition is not always of anomalous type.

Using the same bath, but carrying out the tests at 25 °C (Fig. 8), the trend of the curves appears the same as in Fig. 6. At this temperature value the inhibition of the cobalt ions discharge starts when the zinc percentage in the deposits is about 15%. In this case however, on the contrary to what happens in the operating condition related to Fig. 6, the transition from underpotential to thermodynamic electrodeposition corresponds to the transition from normal to anomalous codeposition. In the range of potentials where the zinc reduces in underpotential conditions, the deposition of Zn–Co alloys is always of normal type. It must be emphasized that, in the range –700 ~ –800 mV, in spite of the high percentage of zinc (higher than 10%), the inhibition of cobalt ions discharge does not occur.

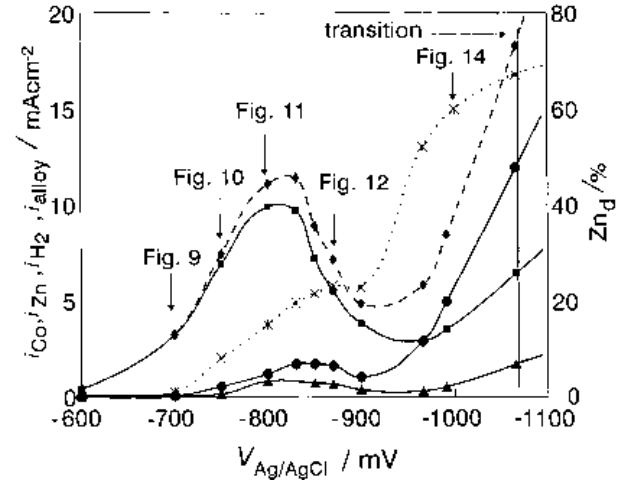

Fig. 6. Effect of the electrode potential on the partial current densities for cobalt (■), zinc (●), H_2 (▲) and alloy (◆) reduction, together with the zinc percentage of deposits (✳). Co_b 30%, $T = 55\,°C$.

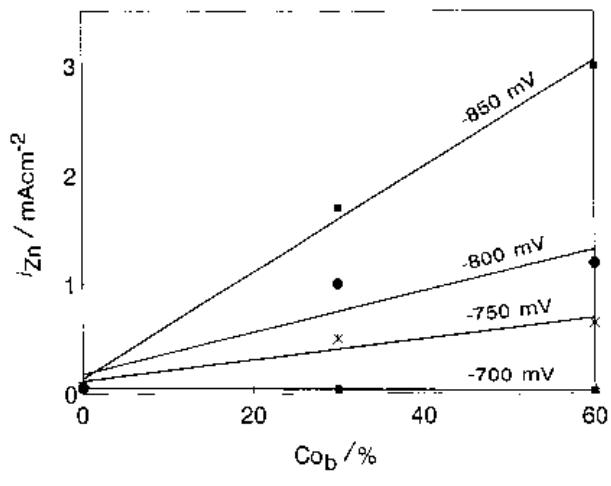

Fig. 7. Effect of the cobalt content of the baths on the zinc partial current density. $T = 55°C$.

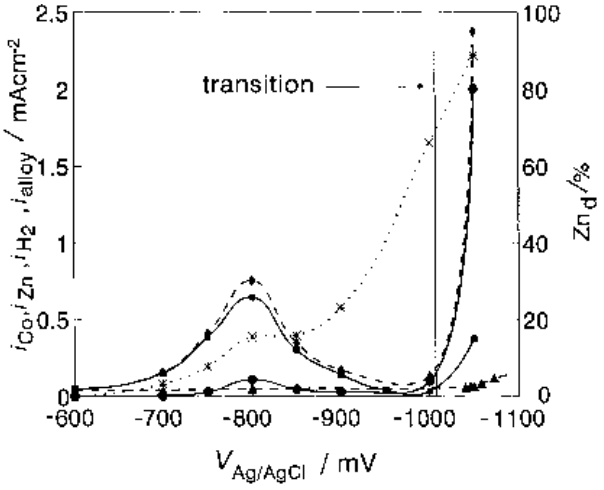

Fig. 8. Effect of the electrode potential on the partial current densities for cobalt (■), zinc (●), H_2 (▲) and alloy (◆) reduction, together with the zinc percentage of deposits (✳). Co_b 30%, $T = 25\,°C$.

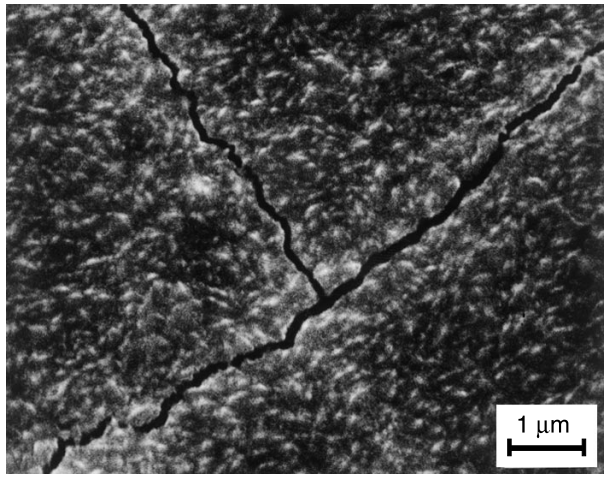

Fig. 10. Microstructure of zinc–cobalt alloy obtained by potentiostatic electrodeposition at –750 mV vs Ag/AgCl. Co_b 30%; $T = 55\,°C$; Zn_d 8%.

The increase in pH at the cathodic interface is generally considered responsible for the inhibition of cobalt discharge in the hydroxide suppression mechanism, as mentioned in the introduction [2, 5]. The present work does not seem to confirm this theory since the partial current density of hydrogen remains quite constant and very low (Figs 6 and 8). Therefore, the inhibition of cobalt ion reduction in these operating conditions does not seem connected with an increase in pH.

The observation carried out by SEM on the surfaces of the deposits obtained at the potential values of Fig. 6, are shown in Figs 9–13. Deposits obtained at –700 mV (Fig. 9, Zn_d 0.5%) are formed of pure cobalt and are not cracked, according to the solubility of Zn in Co, which is less than 3% [18]. The coatings obtained at –750 mV are cracked (Fig. 10, Zn_d 8%); in the range –800 to –830 mV the deposits are cracked and do not adhere to the steel substrate (Fig. 11, Zn_d 14%). At more negative potential values, in the range where the zinc percentage remains quite constant and the partial current density of cobalt decreases, the deposits are still cracked, but they adhere again to the steel substrate (Fig. 12, Zn_d 23%). The cracking of the cobalt deposits with inclusion of zinc above 3% was found by other authors [10, 11]; the higher percentage of zinc in the alloy produces more internal stresses in the deposits, until a change in the crystalline structure occurs which reduces these internal stresses. The maximum in the internal stresses coincides with the maximum in the current density of cobalt (i_{Co}). These deposits show a brittle behaviour with the surface fracture that looks like a vitreous fracture (Fig. 13). At potentials where the zinc can reduce in thermodynamic conditions and the partial current density of zinc becomes higher than the partial current density of cobalt, the deposition of compact and well formed zinc-rich deposits occurs (Fig. 14, Zn_d 60%).

The influence of the electrode potential on the deposition of various phases of different zinc composition from the same electrolyte was also found by

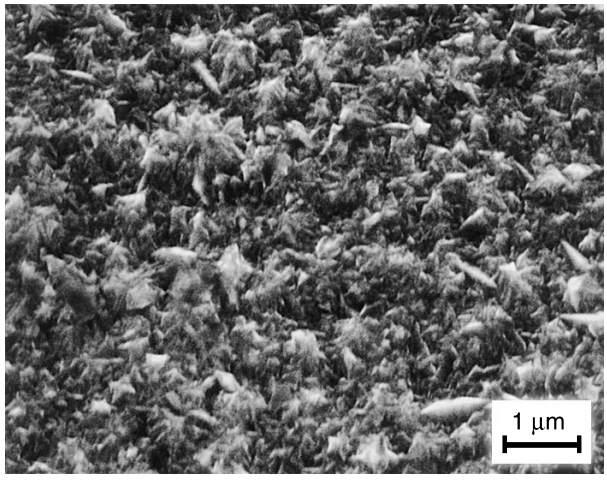

Fig. 9. Microstructure of zinc–cobalt alloy obtained by potentiostatic electrodeposition at –700 mV vs Ag/AgCl. Co_b 30%; $T = 55\,°C$; Zn_d 0.5%.

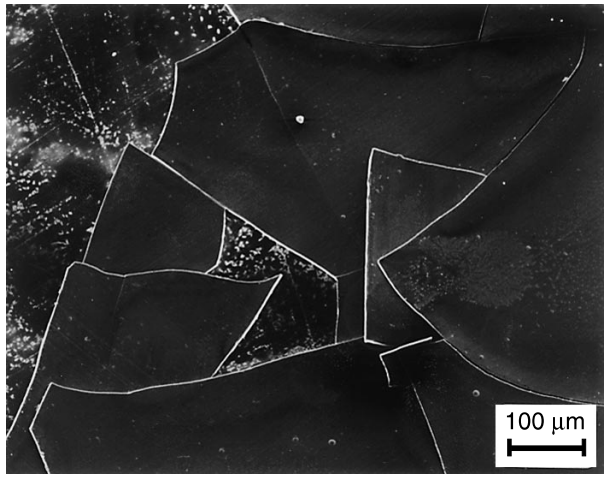

Fig. 11. Microstructure of zinc–cobalt alloy obtained by potentiostatic electrodeposition at –800 mV vs Ag/AgCl. Co_b 30%; $T = 55\,°C$; Zn_d 14%.

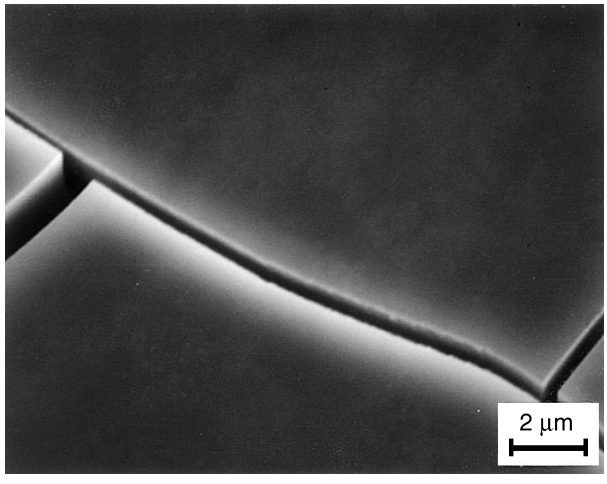

Fig. 12. Microstructure of zinc–cobalt alloy obtained by potentiostatic electrodeposition at –870 mV vs Ag/AgCl. Co_b 30%; $T = 55\,°C$; Zn_d 23%.

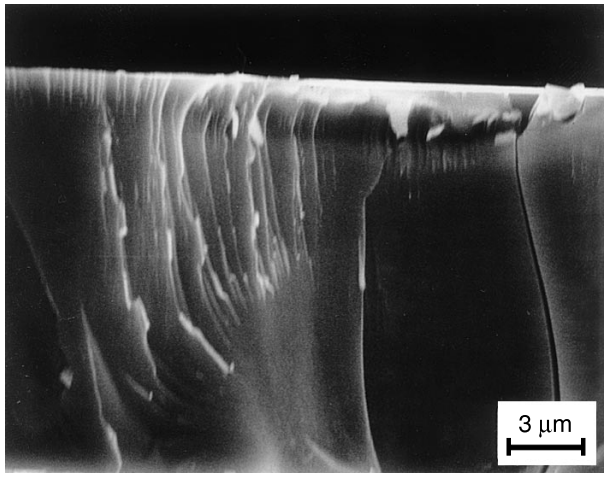

Fig. 13. Fracture of Zn–Co alloy (Zn_d 23%) obtained by bending of the coating layer.

other authors for Zn–Ni and Zn–Co alloys electrodeposition [13, 21].

The X-ray analysis do not always permit to identify the phases present in the coatings (Fig. 15). Deposits of only cobalt are not crystalline, the peaks have very low intensity and can be attributed to low content of crystalline αCo in the quite completely amorphous deposit (Fig. 15, line a).The presence of zinc in the range 0.5 ~ 23% makes the deposits more and more amorphous (Fig. 15 lines b, c, d, e). When the zinc reaches 60%, the deposits become crystalline and the zinc peaks clearly appear (Fig. 15, line f).

4. Conclusions

The deposition of Zn–Co alloys is generally a codeposition of anomalous type, but, in particular electrodeposition conditions, it is possible to obtain normal codeposition.

The shift in potential and in cobalt percentage in the deposits, which occur at a particular current density during galvanostatic electrodeposition, does

Fig. 14. Microstructure of zinc–cobalt alloy obtained by potentiostatic electrodeposition at –1000 mV vs Ag/AgCl. Co_b 30%; $T = 55\,°C$; Zn_d 23%.

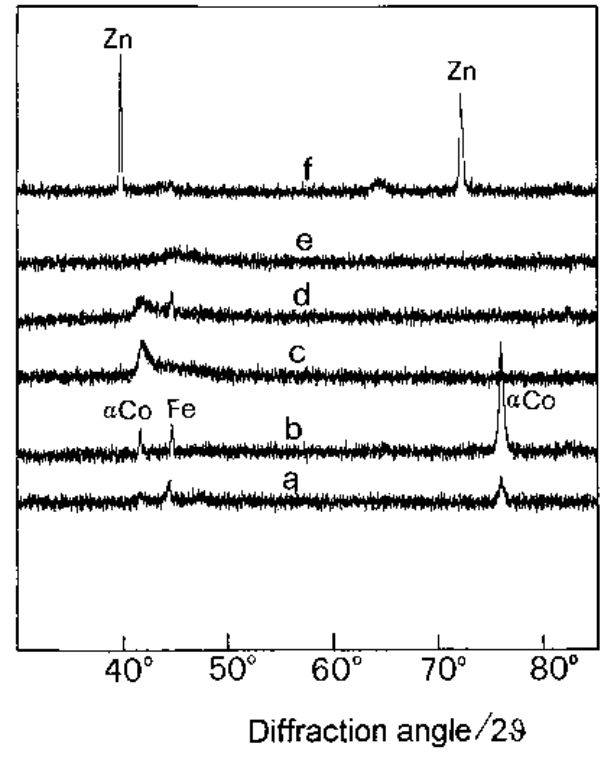

Fig. 15. X-ray diffraction profiles of electrodeposits obtained by potentiostatic electrodepositions: (a) –700 mV, bath without zinc; (b) –700 mV, Co_b 30%, Zn_d 0.5%; (c) –750 mV, Co_b 30%, Zn_d 8%; (d) –800 mV, Co_b 30%, Zn_d 14%; (e) –870 mV, Co_b 30%, Zn_d 23%; (f) –1000 mV, Co_b 30%, Zn_d 23%. $T = 55\,°C$.

not always correspond to the transition from normal to anomalous codeposition. The sharp variations in cathodic potential are due to the zinc ions discharge which passes from underpotential to thermodynamic conditions.

In the underpotential deposition, the electrode potential determines the deposition of various phases of different composition. The inclusion of zinc above 3% causes cracking of the cobalt deposits and the further increase in the percentage of zinc in the alloy produces more internal stresses in the deposits. The

inhibition of the cobalt ions discharge starts only when the zinc percentage in the deposits reaches about 15%. The maximum in the internal stresses coincides with the maximum in the current density of cobalt (i_{Co}).

At potentials where the zinc can reduce in thermodynamic conditions, deposits containing more than 60% zinc become compact and well formed, even when the codeposition is still of normal type.

Acknowledgements

The research was supported by Conselho Nacional de Desenvolvimento Científico e Tecnológico (CNPq), Brasil.

References

[1] A. Brenner, 'Electrodeposition of alloys', vols I and II, Academic Press, New York and London (1963).
[2] K. Higashi, H. Fukushima, T. Urokawa, T. Adaniya and K. Matsudo, *J. Electrochem. Soc.* **128** (1981) 2081.
[3] L. Felloni, R. Fratesi, E. Quadrini and G. Roventi, *J. Appl. Electrochem.* **17** (1987) 574.
[4] L. Felloni, R. Fratesi and G. Roventi, Proceedings of the XXII International Metals Congress, Bologna, Italy (17–19 May 1988), p. 687.
[5] H. Fukushima, T. Akiyama, K. Higashi, R. Kammel and M. Karimkhani, *Metall.* **42** (1988) 242.
[6] R. Albalat, E. Gómez, C. Muller, M. Sarret, E. Vallés and J. Pregonas, *J. Appl. Electrochem.* **20** (1989) 529.
[7] R. Albalat, E. Gómez, C. Muller, M. Sarret, E. Vallés and J. Pregonas, *ibid.* **20** (1990) 635.
[8] R. Fratesi and G. Roventi, *J. Appl. Electrochem.* **22** (1992) 657.
[9] H. Dahms and I. M. Croll, *J. Electrochem. Soc.* **112** (1965) 771.
[10] J. Mindowicz, C. Capel-Boute and C. Decroly, *Electrochim. Acta* **10** (1965) 901.
[11] M. Yunus, C. Capel- Boute and C. Decroly, *ibid.* **10** (1965) 885.
[12] M. I. Nicol and H. I. Philip, *J. Electroanal. Chem.* **70** (1976) 233.
[13] S. Swathirajan, *ibid.* **221** (1987) 211.
[14] R. Fratesi and G. Roventi, *Mater. Chem. Phys.* **23** (1989) 529.
[15] R. Piontelli, *in* 'Atlas of Electrochemical Equilibria in Aqueous Solutions' (edited by M. Pourbaix), NACE, Huston, Texas (1974), p. 11.
[16] M. F. Mathias and T. W. Chapman, *J. Electrochem. Soc.* **134** (1987) 1408.
[17] *Idem, ibid.* **137** (1990) 102.
[18] C. Karwas and T. Hepel, *J. Electrochem. Soc.* **136** (1989) 1672.
[19] M. Pushpavanam and K. Balakrishnan, *J. Appl. Electrochem.* **26** (1996) 283.
[20] M. Maja, N. Penazzi, R. Fratesi and G. Roventi, *J. Electrochem. Soc.* **129** (1982) 2695.
[21] M. L. Alcalá, E. Gómez and E. Vallés, *J. Electroanal. Chem.* **370** (1994) 73.